

Strain and fabric development in a buckled calcite vein and rheological implications.

PETER HUDLESTON AND JOHN TABOR

Hudleston, P.J. and Tabor, J.R. 1988 12 30: Strain and fabric development in a buckled calcite vein and rheological implications. *Bulletin of the Geological Institutions of the University of Uppsala*, N.S., Vol. 14, pp. 79–94. Uppsala. ISSN 0302-2749.

Information about natural folding processes and rock rheology can be obtained by the study of fold shape, strain, and fabric. Folds in fibrous antitaxial veins within slates of the Canyon Creek Formation west of Golden, British Columbia, Canada, display characteristics of buckle folds – constant vein thickness, preferred wavelength, and a rapidly decaying zone of contact strain away from the folds into the slates. The original orthogonality between fibres and the vein walls has been maintained during buckling, indicating coaxial strain paths at all points around the folds. This rules out flexural flow and suggests tangential-longitudinal strain as the deformation-accommodating process. However, the primary antitaxial suture in the vein remains nearly centrally positioned passing from limb to hinge of each fold and is not significantly displaced towards the outer arc as required by tangential-longitudinal strain. This, together with the absence of radial extensional veins in the outer arc and the presence of radial tectonic stylolites and pressure solution films in the inner arc, suggests that folding to high amplitude was accommodated to a significant extent by inner arc collapse and removal of calcite by pressure solution.

Despite the overall simplicity of the coaxial strain paths, on the scale of individual fibers deformation is inhomogenous. Calcite c-axes are initially preferentially parallel to the fibers. Conjugate twinning in all grains occurred during layer-parallel shortening prior to significant fold amplification, secondary twinning occurred within many primary twins and, towards the inner arc where total shortening strains are highest, most grains have been completely twinned, resulting in optic axes at high angles to the fibers. In addition, twin planes have been systematically rotated, indicating translation gliding (on r or f slip systems). This becomes increasingly important towards the inner arc. There is also evidence locally for slip sub-parallel to the fibers, in the form of wedging in the inner arc, giving alternate senses of slip.

The mean ratio of wavelength (arclength of mature folds) to thickness of the folds (7.0), combined with the limited layer-parallel shortening, provides estimates of parameters in buckling theory, and leads to the conclusion that the flow law of calcite was significantly non-linear during folding, with power law exponent > 3 , and perhaps > 10 .

P.J. Hudleston & J.R. Tabor, Department of Geology and Geophysics, University of Minnesota, Minneapolis, MN 55455, USA. Received 24th April 1987, revision received 8th February 1988.

Introduction

Under appropriate circumstances, it is possible to gain information about the kinematics of deformation and the mechanical properties of rocks during slow natural deformation from a study of folds. If exposure is sufficient and if suitable markers are present, it is possible to determine whether folds formed as a result of buckling, bending, or passive amplification (e.g. Hudleston, 1986) and to determine how well the strain pattern matches idealized models of tangential-longitudinal strain or flexural slip (Ramberg, 1963). If the folds are buckles, it may be possible to derive information on viscosity contrasts and the nature of the flow law

followed by the rock types involved. This cannot be done with great precision, but it is important to make efforts to do this because there is considerable uncertainty in extrapolating flow laws derived from experimental work to natural strain rates some six to eight orders of magnitude slower (e.g. Paterson, 1987). We extend in this paper a study reported earlier by Hudleston and Holst (1984) on buckled limestone layers in slates. In that study wavelength and thickness were measured for a large population of folds, and clasts in a limestone bed were used to determine strain and thus to estimate the amount of shortening accompanying buckling. Buckling instability is very sensitive to the exponent in a flow law of power law type, and the amount of layer-

parallel shortening, combined with knowledge of wavelength/thickness ratios, allows the value of the exponent to be estimated (Hudleston and Holst, 1984). In the earlier study shortening turned out to be small, leading to the conclusion that the buckled layer followed a non-linear flow law.

In this study, we examine the geometry and fabric of folds developed in antitaxial calcite veins in slates. As we will show, this leads to similar conclusions about the buckling instability as the earlier study, and it also provides detailed information on the strain pattern and mechanisms of deformation active during buckling.

Description of Folds

The folds studied outcrop 25 km northwest of Golden, British Columbia, in the Canyon Creek Formation. The veins in which they occur are subparallel with bedding and both dip steeply south (Fig. 1).



Fig. 1. Photograph of folded calcite veins in slates of the Canyon Creek Formation, 25 km northwest of Golden, British Columbia, exposed in a roadcut on Canadian Highway 1. Slaty cleavage dips steeply ENE.

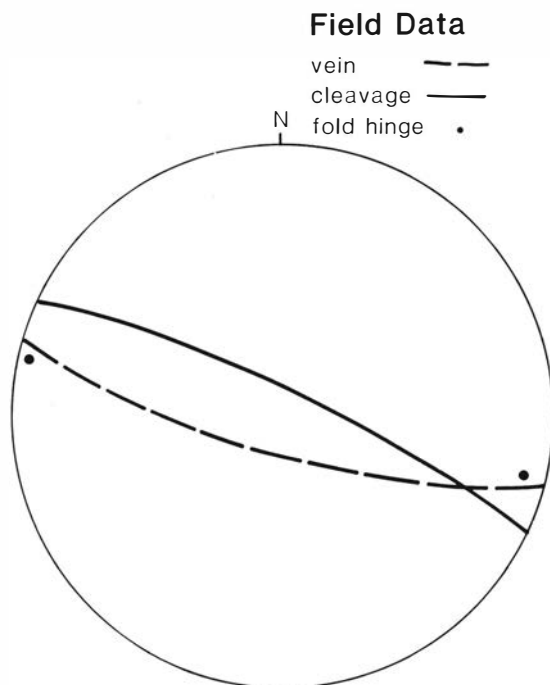


Fig. 2. Structural data for the studied folds shown in Fig. 1 plotted in lower hemisphere equal-area projection. The plane representing the veins is the enveloping surface to the folds. The cleavage is that measured away from the disturbance due to folding. Two separate fold hinges are shown, as measured in outcrop.

A good cleavage in the slates hosting the veins formed synchronously with the folds and dips steeply north, and the intersection of bedding and cleavage is subhorizontal and sub-parallel to the minor fold hinges in the veins (Fig. 2). The folds are asymmetrical, but not markedly so considering the small angle between cleavage and layering. The axial surfaces of the folds occupy a position intermediate between perpendicular to the enveloping surface and parallel to regional cleavage, and cleavage is refracted close to the folded vein. Visual inspection shows most folds to be sub-parallel in shape (class 1B of Ramsay, 1967), but measurement of the fold selected for detailed study (Fig. 3) shows it to be class 1C, with a modest amount of thinning in the limbs (Fig. 4).

It is very useful to know the distribution of normalized wavelengths for a population of folds. The procedure used involves measuring the distance between two adjacent hinges (along either bounding surface or center of the layer); this quantity is the arclength of a "half-wavelength unit" (Hudleston, 1973). Arclength and thickness were measured on

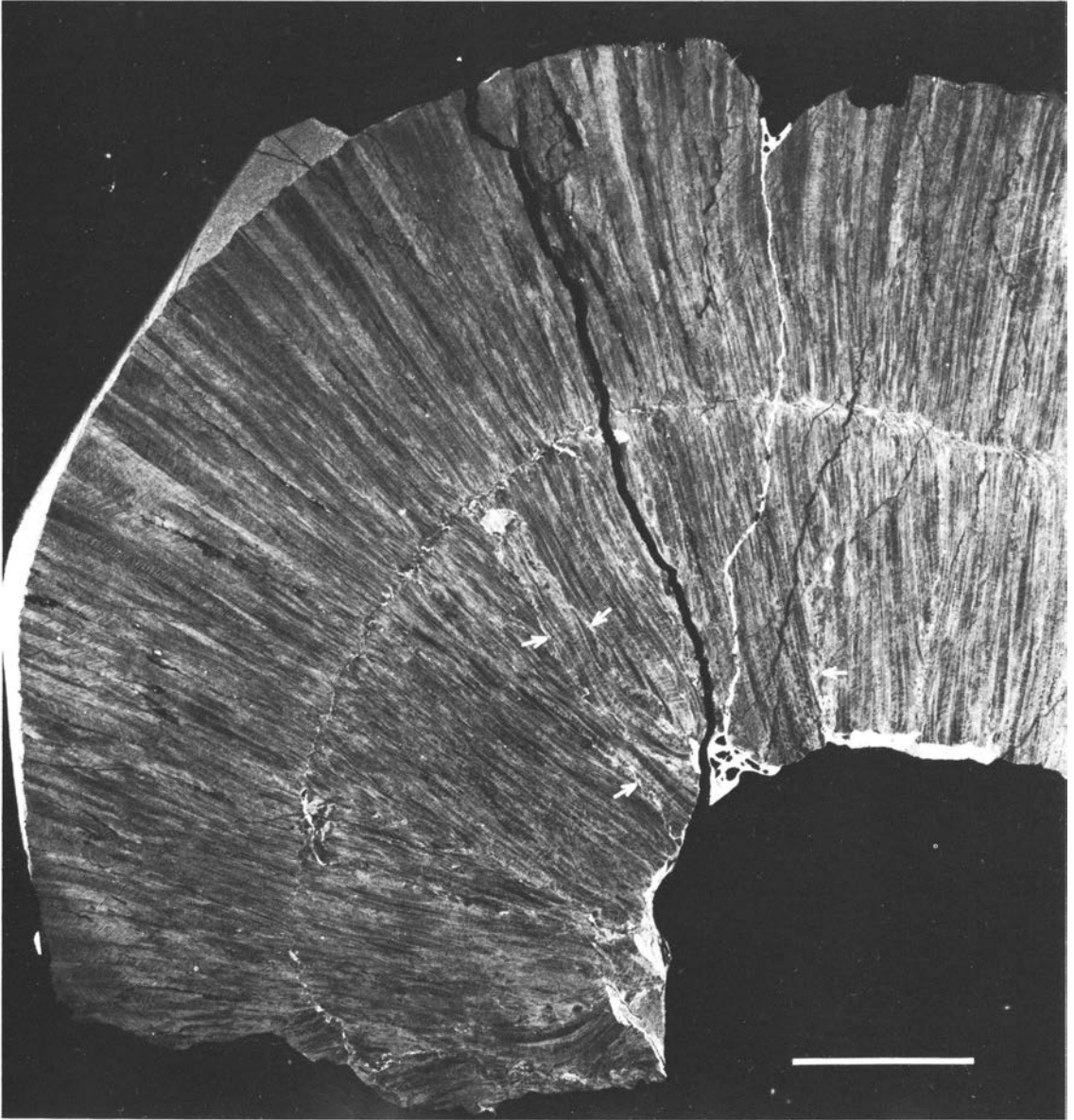


Fig. 3. Negative print of thin section of the folds in an antitaxial calcite vein selected for detailed study. Note the fibers nearly orthogonal to the vein walls and the median antitaxial suture, with local deviations. Selected pressure solution surfaces indicated by arrows. Scale bar is 0.5 cm.

the outcrop or on photographs (taken with the camera sighted along the fold hinge) of surfaces approximately perpendicular to the fold hinges. The quantity $L = 2 \times \text{arlength}/\text{thickness}$ is recorded for each half-wavelength unit. The average 'wavelength'/thickness ratio (\bar{L}) for 22 folds in the outcrop studied is 7.0, which is very similar to the average (7.1) obtained for measurements of 212 folds in

veins or layers in a 15 km traverse across the western ranges of the Canadian Rockies, just to the east of the Rocky Mountain Trench and the location of the folds described here (Hudleston and Holst, 1984).

Calcite 'fibers' are well preserved in all veins, and there is usually a suture present, normally in the center of the veins and outlined by an insoluble resi-

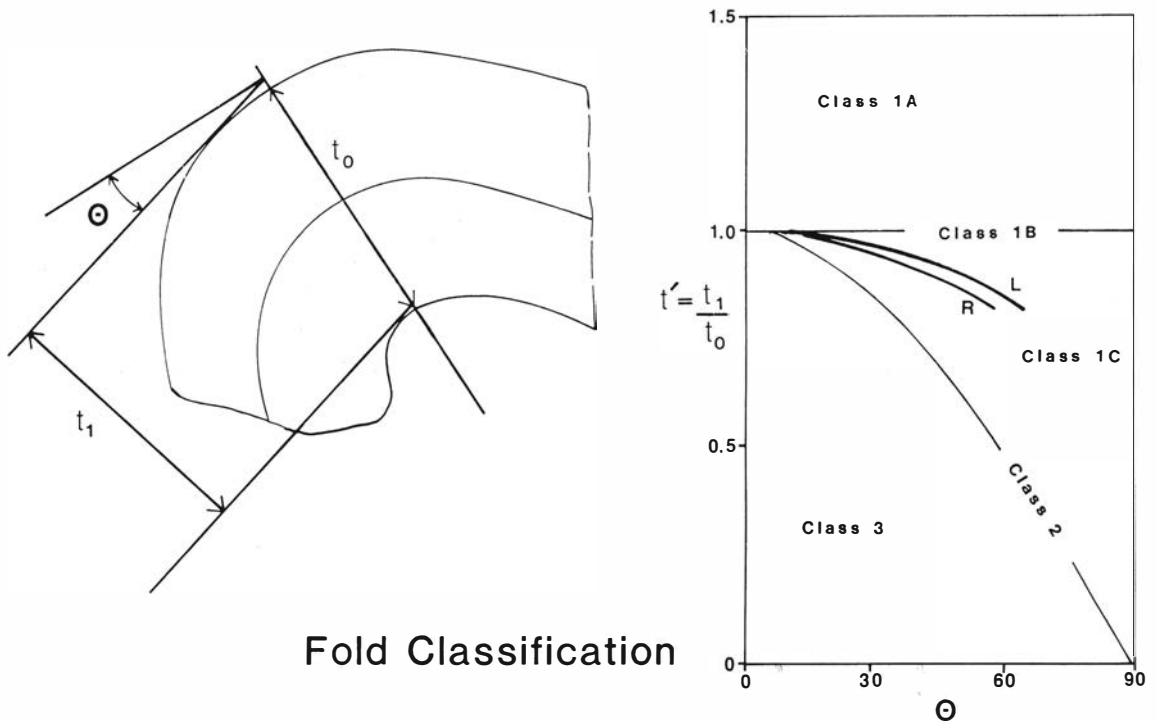


Fig. 4. Thickness variations from hinge to limbs of the selected fold, measured in a section perpendicular to the hinge. R and L are thickness variations measured in the right and left limbs respectively of the studied fold in Fig. 3.

due. The different composition of the veins and host rock, the preservation of fragments of wall rock within the veins, and in particular the thickening of fibers and decrease in their numbers (as unfavorably oriented fibers were eliminated during growth) away from the suture in the relatively undeformed fold limbs indicates these are antitaxial veins (Fig. 3).

Strain Pattern

There are two features that provide information on the state of strain within the folded veins. The first is the combination of calcite fibers and the layer boundaries and antitaxial suture, which represent an originally orthogonal grid prior to folding. The second is the twinning within the fibers. The orientation and thickness of the twins can be measured to provide an estimate of strain, following the method developed by Groshong (1972, 1974).

The most striking mesoscopic feature of the folds is that the fibers remain nearly normal to the vein boundaries and antitaxial suture around the folds

(Fig. 3). This implies that these directions are the directions of principal strain, and that the strains in the folds developed everywhere coaxially, or nearly so. Thus the folds provide an excellent example of a coaxial, rotational deformation (e.g. Lister and Williams, 1983). The pattern of fibers is obviously more consistent with tangential-longitudinal strain (TLS) than with flexural slip (Fig. 5). A second important feature is that the antitaxial suture lies nearly at the center of the vein in the fold hinges. It is not greatly displaced towards the outer arc as would be the case in two-dimensional tangential-longitudinal strain. A brief divergence to discuss the theoretical details of such a displacement is in order.

In tangential-longitudinal strain, the stretch parallel to layering (and in plane strain the radial stretch also) are simple functions of distance from the neutral surface and curvature of the neutral surface (Ramsay, 1967, p. 397–400). A line must be selected as the neutral surface before it is possible to construct a fold, however. If the middle line in the undeformed state is so selected, the corresponding material line in the deformed state will obviously lie closer to the outer arc than the inner arc as a result of the strain. But one might also choose as a neutral

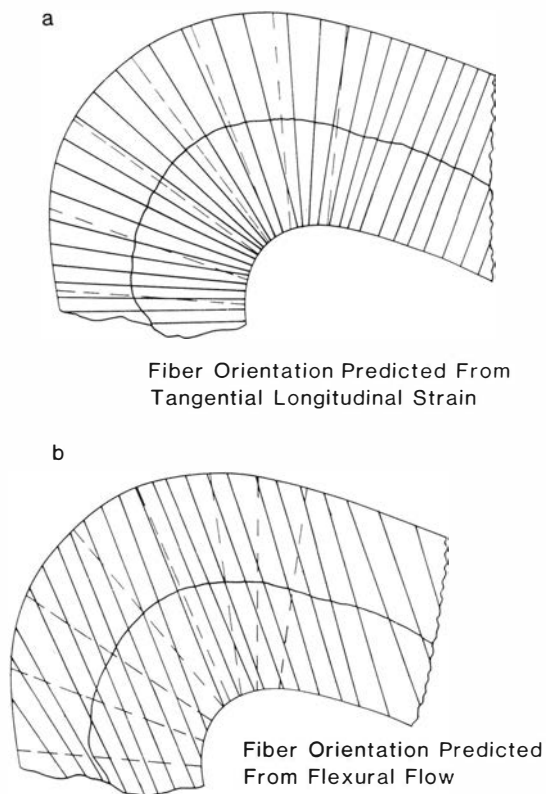


Fig. 5. Predicted pattern of fibers in a folded vein in which strain is accommodated by a) tangential longitudinal strain, b) flexural slip. Actual fiber orientations indicated by dashed lines.

surface the material line in the center of the layer in the folded state. This line will lie closer to the inner arc of the fold-to-be in the unfolded state. It turns out that the second procedure is the more reasonable one, as the following analysis shows.

It is clear that an additional assumption must be made if the location of the neutral surface is to be predicted rather than arbitrarily assumed. A reasonable assumption is that the neutral surface takes up a position that minimizes the work done in distorting the layer. Because we don't know a priori the form of the constitutive relationship, the most reasonable procedure is to calculate the natural octahedral unit shear, $\bar{\gamma}_{os}$ (Nadai, 1963, p. 73). This is directly related to the work done in deforming a purely plastic material. With a given fold shape, $\bar{\gamma}_{os}$ can be integrated across the layer from inner to outer arc, for each possible neutral surface position. This has been done for a shape given by circular arcs, and integrated $\bar{\gamma}_{os}$ as a function of initial neutral surface position for five different values of

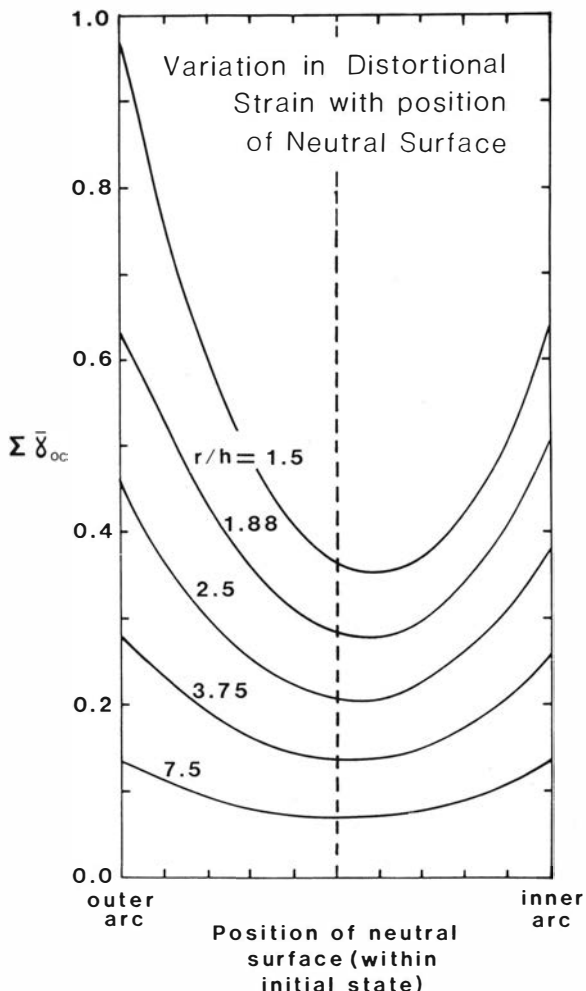


Fig. 6. Plots of integrated natural octahedral unit shear, $\bar{\gamma}_{os}$, as a function of position of the neutral surface in the unfolded state, for various values of, r/h radius of curvature (of the middle of the layer) divided by thickness.

radius of curvature/thickness (r/h) is plotted in Fig. 6. This figure shows that the position of the neutral surface that minimizes the distortion progressively shifts away from the center of the layer towards the inner arc as the radius of curvature is decreased. If the radial positions of the points in Fig. 7 are recalculated to reflect the deformed or folded state, the minima in all cases lie at the centers of the layers. Thus the predicted position of the neutral surface is the *central line* in the *deformed state*. The material line originally in the middle of the layer will lie progressively further towards the outer arc in the deformed state, as radius of curvature is decreased. The predicted position of this line is plotted in Fig.

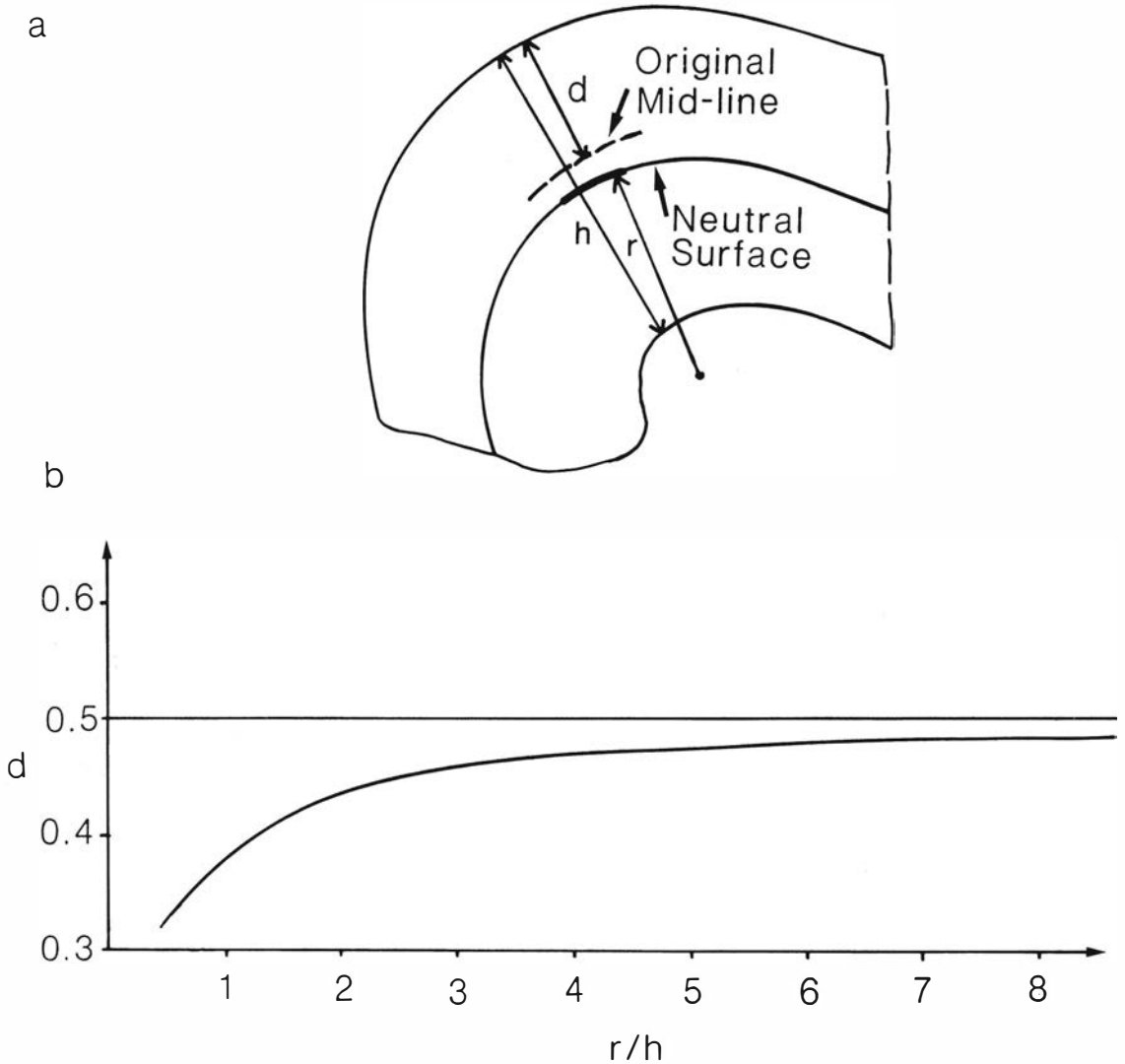


Fig. 7. Calculation of the position of the material line initially at the middle of the layer (roughly equivalent to the suture in the studied fold) after folding, assuming that the neutral surface lies in the middle of the layer in the deformed state, with deformation accommodated by tangential longitudinal strain. a) Definition of terms; b) Plot of d , the distance from the outer arc to the originally central material line in a layer of unit thickness, against r/h .

7. Progressive folding to maintain least work implies migration of the neutral surface across the layer.

Returning to the studied fold, what are we to make of the fact that the median line is not significantly displaced towards the outer arc of the fold (Fig. 8), as predicted in the above analysis? There seem to be three possibilities. The first is that the strain might not be two-dimensional (or more specifically might deviate from a constant extension or contraction in the third dimension), in that material could have been extended parallel to the hinge in

the inner arc to compensate for the space problem associated with large shortening perpendicular to the axial plane, and perhaps shortened in the outer arc, as in anticlastic bending (Ramsay, 1967, p. 402). However, this is probably not significant because, although the three-dimensional forms of the folds could not be studied well, they do not appear to be significantly non-cylindrical, as would be required if this local stretching and contraction in the third dimension were significant. Also, calcite twin data do not support this. The second possibility is

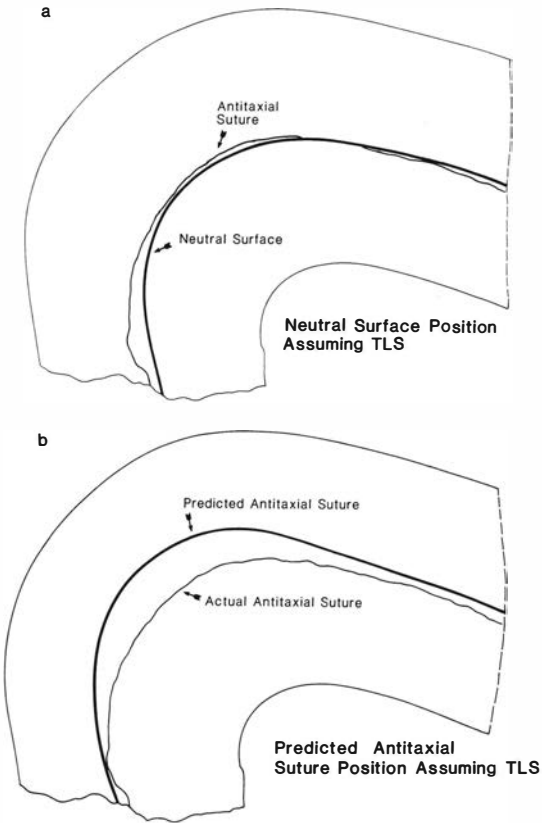


Fig. 8. Comparing a) the predicted and observed positions of the antitaxial suture for the selected fold, and b) the position of the antitaxial suture with the predicted neutral surface, for tangential-longitudinal strain (TLS).

that the antitaxial suture was originally closer to the inner arc than the outer arc. The third possibility, supported by microstructural features to be described later, is that there has been removal of material from the inner arc by pressure solution. This was also an important feature of the folds in the clastic limestone bed studied earlier (Hudleston and Holst, 1984).

Strain from Calcite Twins

Examination of the folded vein in thin section shows an abundance of twinning in the calcite fibers. This provides us with a means of estimating preferred directions of 'compression' and 'tension' around and across the folded layer, using the method of dynamic analysis developed by Turner (1953) (see also Turner and Weiss, 1963, p. 241–243), and also

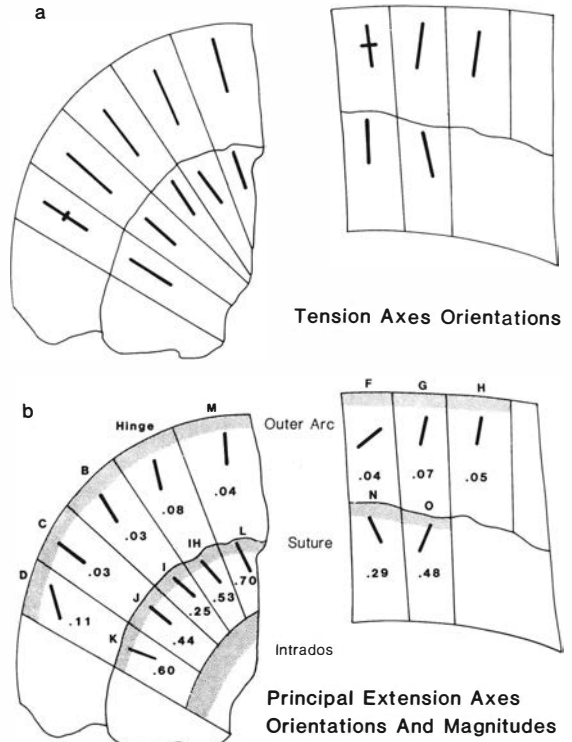


Fig. 9. a) Orientations of 'tension' axes in domains in the outer arc of the fold and just below the suture determined using Turner's (1953) dynamic analysis of calcite twins. b) Orientation and magnitude of the maximum extension, e_1 , of the strain associated with twinning, measured using Groshong's (1972) strain gauge technique. The principal directions (e_1) all lie very close to the plane of the figure (perpendicular to the fold hinge). The domains are indicated by stippling and are separated by the radial lines shown. The strain magnitudes at the suture are unreliable. No strain magnitudes were calculated for the intrados.

of measuring the strains due to twinning, using the strain gauge technique of Groshong (1972).

Calcite c-axes and poles to e twin lamellae were measured by standard techniques (e.g. Turner and Weiss, 1963, p. 197) using a universal stage in two traverses along the arc of the selected fold, one traverse near the outer arc and one just below the median line (Fig. 9a). The overall directions of preferred 'extension' in each of several domains bounded by radii to the fold are shown in Fig. 9. Each domain contained from 15–20 grains. Thickness of twin lamellae and host grain were also measured in thin section and, together with orientations of host crystals and poles to twin lamellae, these provided the data needed to calculate the strain in each domain due to twinning. The results are shown in Fig. 9b.

The general pattern of maximum principal extensional strain and 'tension' axis orientations shown in the two figures is quite clear. There is a radial extensional strain of between 3 and 10 % in the outer arc. The principal strains lie close to the profile plane of the fold, and in general they are parallel or perpendicular to the vein walls and the suture. There is thus a general consistency between the observation that the fibers remained perpendicular to the vein walls during folding and the measured strain data that indicate principal strains are parallel or perpendicular to the fibers. In domain F (and to a lesser extent in domain D), there are a few twins indicating extensions parallel to the layer, and these are responsible for the deviant orientations of e_{\max} in these domains (compare Figs. 9a and 9b).

The values of twin strain magnitude are most reliable in the outer arc, where twinning is least intensely developed. The situation is not as straightforward in the inner arc, where it becomes difficult to separate twin from host, and where twin lamellae and host c-axes become rotated due to translation gliding. This latter effect violates an assumption of the strain gauge method, which allows for no lattice rotation (except due to twinning within the twins) and no translation gliding on other slip systems. The significance of the lattice and twin rotations is discussed in detail in a later section. There is an additional violation of the assumptions of the method in that the strain magnitudes are large in the inner arc, whereas the method of analysis makes use of infinitesimal strain theory. Groshong (1972) discussed the effects of assuming infinitesimal strain on the calculated principal strains, and he considered the resulting errors in magnitude and orientation acceptable (they are within a few percent and a few degrees) below the practical limit for using the method, which he took to be when grains are 50 % twinned. A 50 % twinned grain (on one twin set) has a maximum extension (e_{\max}) of 19 % (in a direction 23° to the c-axis of the host), and if a grain is 50 % twinned on each of two twin sets, e_{\max} is 28 % (in a direction at 4° to the c-axis of the host). Little significance should be attached to the strain magnitudes in the inner arc along the suture shown in Fig. 9b. The important thing to note is that strain is larger than in the outer arc, but of similar orientation.

Another reason for exercising caution in interpreting the values and orientations of the principal strains (Fig. 9b) is that the number of grains in each domain and the range in orientations of the c-axes of the host grains are small, limiting the strains that can develop and giving rise to possible non-correspondence between principal directions of stress and strain.

Analysis of Folding

Folds in the veins display all the characteristics of buckles: thickness remains fairly constant from hinge to limbs, there is a preferred wavelength/thickness ratio, there is a zone of contact strain decaying rapidly away from the vein into the slates (Ramberg, 1963, Hudleston, 1986), and the cleavage in the host rock in the inner arcs of the folds is subparallel with the axial surfaces. The orientations of the calcite fibers and principal strains due to twinning are as expected for tangential longitudinal strain, in that they are parallel or perpendicular to the vein walls – a pattern predicted for strain in buckled competent layers and observed in experiments (e.g. Ramberg, 1961, 1963), but the magnitudes of the strains due to twinning and the lack of

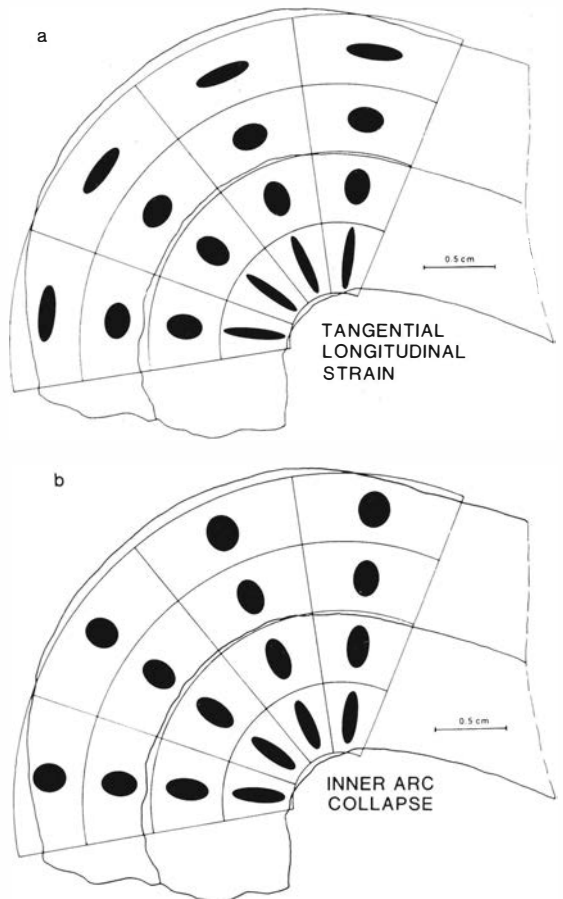


Fig. 10. Idealized patterns of strain in parallel fold of circular arcs, approximating the shape of the studied fold (bold lines). a) Tangential longitudinal strain. b) Collapse of inner arc by volume loss, with the outer arc as the neutral surface.

significant outward deflection of the antitaxial suture in the hinges of the folds are both inconsistent with tangential longitudinal strain (Fig. 9b and 10).

The lack of cumulative or incremental extensional strains or extensional veins in the outer arc of the fold, the minimal deflection of the antitaxial suture in the vein from a central position, and the presence of radial pressure solution films and stylolites in the inner arc all point towards a process of inner arc collapse by pressure solution removal of material (Fig. 10). The existence of layer-parallel compressional strains in the outer arc of the fold and in the limbs are interpreted to be the result of uniform layer-parallel shortening prior to significant amplification of the buckles (Biot, 1961, Sherwin and Chapple, 1968). It is assumed that all the strain recorded by the calcite twins in the outer arc occurred during this early phase of deformation. Shortening is thus taken to be between 3–10 %, corresponding to a strain ratio, T , in the profile plane of the folds of between about 1.05 and 1.2. Allowing for at least 30 % error in the measurements (Groshong, 1974), and noting that the strain cannot be significantly less than given by a value of $T = 1.05$ with the amount of visible twinning, it seems reasonable to take T to lie in the range $1.05 < T < 1.3$.

Note that there *must* be some fiber-parallel extension in the inner arc associated with the more intensive twinning that occurred there during fold growth to high amplitude. This is incompatible with no outward deflection of the antitaxial suture. This may be explained by the suture being originally slightly offset from the center towards the inner arc and by the total removal by pressure solution of the innermost part of these fibers in the fold core, thus losing the original edge of the vein. These could counteract the effect of up to about 30 % extension of the fibers.

The higher twin strains recorded in the inner arc accumulated during growth of the fold to high amplitude, in orientations consistent with tangential longitudinal strain, but with magnitudes much less than predicted because of the simultaneous and important removal of material by pressure solution. The few twins consistent with layer-parallel extension in the outer arc must have developed during this later stage of folding (domains D and F, Fig. 9b). There probably would have been larger extensional strains developed during this stage but for the fact that the preferred orientation of calcite c-axes is perpendicular to the vein, placing most grains in positions unfavorable for twin gliding in layer extension (note that twin gliding on e can only be in one sense).

With layer-parallel shortening in the range $1.05 < T < 1.3$, and a value for \bar{L} of 7, we may use the

results of buckling theory to find estimates of viscosity ratio and power law exponent (Fletcher, 1974). The analysis follows closely that described in detail in Hudleston and Holst (1984), and the procedures will not be repeated here. Suffice to say that the theoretical formulation of Fletcher (1974) for power law rheology is followed, and that the theory predicts, for a given viscosity ratio and power law exponents of layer and matrix, that there exists a harmonic component (in a spectrum of components that represent the interface between layer and matrix) that is most amplified. This is represented by L_d , the dominant wavelength/thickness ratio which is a function of T , the amount of layer shortening. Fletcher and Sherwin (1978) have shown empirically that \bar{L} is a good approximation of L_d provided the initial amplitude spectrum of irregularities in the interface between layer and matrix is one of white roughness. Buckling instability is highly sensitive to the power law exponent for the stiff layer, but insensitive to the exponent for the matrix, which is here set equal to 1 and not discussed further. In applying the theory it is assumed that $L_d \approx \bar{L}$, and also that the measured shortening in the outer arc of the layer occurred during wavelength selection, and that the spectrum of L became frozen in when this shortening ceased.

The data set $L_d = \bar{L} = 7.0$ and $1.05 < T < 1.3$ is not compatible with Newtonian layer behavior. For such a rheology, thin plate theory (Sherwin and Chapple, 1968) yields a viscosity ratio of 9–12 and maximum amplifications of < 5 .

If a power law rheology is assumed, estimates of amplification of the dominant wavelength harmonic component must be made. Various lines of reasoning suggest this will be in the range $5 < A_{\max} < 100$ (Hudleston and Holst, 1984). The relationship among dominant wavelength, shortening, viscosity ratio, and power law exponent for an amplification of $A_{\max} = 20$ are shown in Fig. 11. For $L_d = 7.0$ and $T = 1.05$, we find $n \approx 40$, and $Q \approx 0.03$ (corresponding to a viscosity ratio of $\mu_L/\mu_M = 200$), and for $L_d = 7.0$ and $T = 1.3$, we find $n \approx 5$ and $Q \approx 0.05$ (corresponding to a viscosity of $\mu_L/\mu_M = 50$). Varying L_d by one standard deviation gives estimates within the stippled field shown in Fig. 11. Another way of representing the theoretical relationship and the data is shown in Fig. 12, in which layer-parallel shortening is plotted against power-law exponent for a fixed value of L_d and various values of amplification. Again, the range of estimates of n are all > 3 . If the initial amplitude spectrum is not one of white roughness, but rather one of constant amplitude (Fletcher and Sherwin, 1978, Hudleston and Holst, 1984), \bar{L} underestimates L_d by an amount that depends on the dispersion of the distribution.

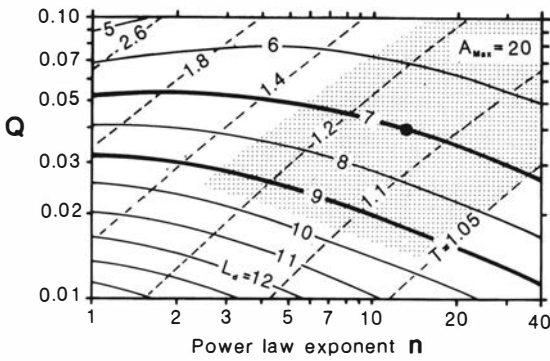


Fig. 11. Theoretical relationship between rheological parameter, $Q = (\mu_M/\mu_L)n^{1/2}$, and power law exponent, n , for various values of dominant wavelength, L_d , at constant amplification, $A_{max} = 20$. Contours of shortening, T , are also shown. Probable values of L_d and T for the studied folds lie in the stippled region. The dot represents the average value of L and T .

For our set of data, dispersion is equal to 0.39 and, using the Fletcher and Sherwin (1978) empirical relationship, $\bar{L}/L_d = 0.76$, giving $L_d = 9.0$. This is shown as a solid line in Fig. 11. Such a value of L_d leads to somewhat lower estimates of the power-law exponent.

To the extent that pressure solution has removed material from the inner arcs of the folds, the present arc lengths (as measured) will be less than the arc lengths at the end of the stage of more or less uniform layer-parallel shortening during which wavelength selection occurs. Thus, the measured values of L , and hence \bar{L} , underestimate the required values for this analysis. If there is no extension of

the outer arc during fold growth to high amplitude, the appropriate measure of arc length is from inflection point to inflection point along the outer arc of the folds, switching sides of the vein at each inflection point. If a correction for this is made \bar{L} is increased by 15–20 % and, for an initial amplitude spectrum of white roughness, L_d increases to 8–8.5, and estimates of n are correspondingly slightly reduced (Fig. 11).

There is a considerable uncertainty in the value of n estimated using buckling theory, due to errors in the measurements of L and T , the nature of the initial amplitude spectrum, and deviations of the natural buckling from the theoretical conditions of constant volume and plane strain. It is impossible to evaluate the effects of all these (however, see the discussion in Hudleston and Holst, 1984), but it is hard to escape the conclusion that buckling of the calcite vein very probably followed a highly non-linear flow law.

Microfabric Analysis

A detailed analysis of the microfabric was undertaken in order to determine the deformation mechanisms responsible for the strain that accommodated the folding, to look for transitions in mechanisms across the fold related to variations in strain intensity, and to determine how individual fibers responded to the deformation. Identification of the deformation mechanisms leads to further predictions concerning the probable form of the flow law obeyed by the calcite during folding. The analysis was done with a petrographic microscope equipped with a universal stage. Orientations of $\{0001\}$ and poles to $\{01\bar{1}2\}$ were measured, in thin sections cut perpendicular to the hinge of the fold, along the: 1) outer arc, 2) inner arc adjacent to the suture, 3) intrados, and 4) length of individual fibers radially across the hinge of the fold (Fig. 9). These data were interpreted in light of the well-known laws on twinning (e.g. Turner and Weiss, 1963, p. 299) and translation gliding (e.g. Turner et al., 1954; Turner and Weiss, 1963; Turner and Orozco, 1976).

Twins are the most prominent component of the microfabric throughout the fold (Fig. 3). They are present in all fibers and most fibers have more than one twin set. However, both the intensity of twinning and the angle between twin plane and fiber length (Figs. 3 and 13 respectively) appear to change across the fold from extrados to intrados. The details of these and other changes are first described and then interpreted in light of the deformational history inferred for the buckle fold.

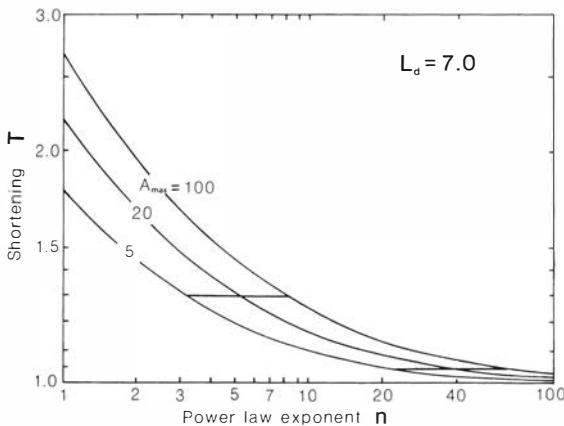


Fig. 12. Theoretical relationship between amount of layer-parallel shortening and power law exponent for $L_d = 7$ at various amplifications. Probable conditions of buckling for the studied folds lie within the stippled area, assuming initial irregularities have spectrum of white roughness.

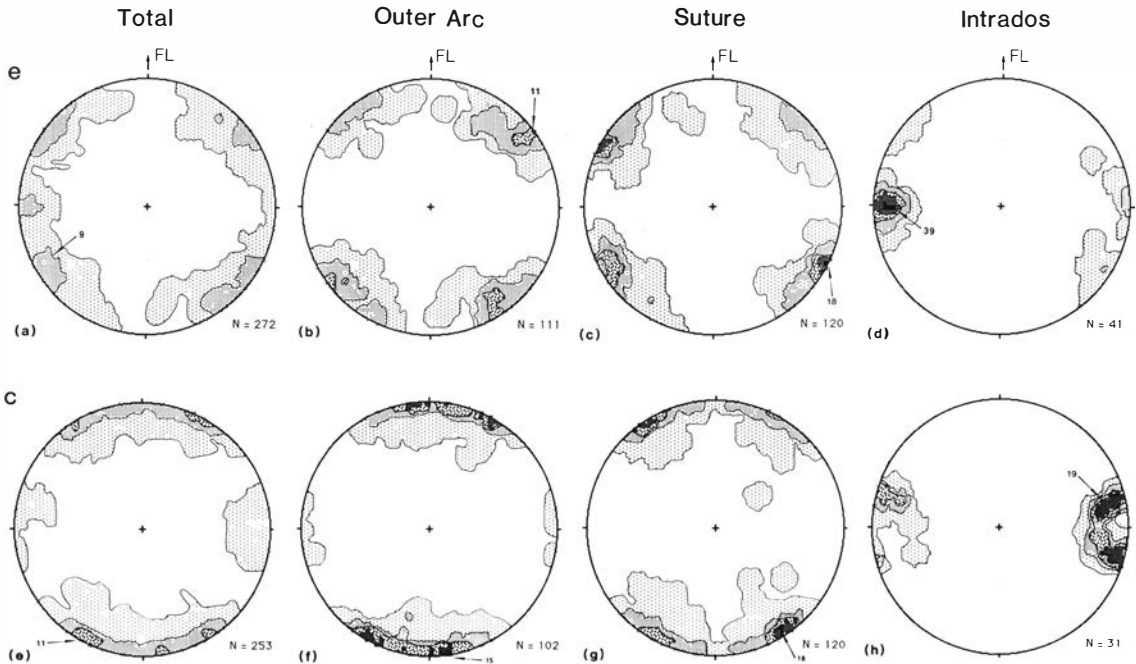


Fig. 13. Contoured equal-area lower-hemisphere projections of poles to $\{01\bar{1}2\}$ (top row) and $[0001]$ axes (bottom row) for three different radial positions in the studied fold (see Fig. 9b). Data for all domains at each radial position are combined by 'unfolding' the fold. The fold hinge is vertical. FL = fiber long axis, N = number of data points. Contour intervals are in a) at 4 and 9 % per 1 % area, b) at 4, 8, and 11 % per 1 % area, c) at 4, 8, 12, 16, and 18 % per 1 % area, d) at 9, 17, 25, 33, and 39 % per 1 % area, e) at 4, 8, and 11 % per 1 % area, f) at 4, 8, 12, and 15 % per 1 % area, g) at 4, 8, 12, 16, and 18 % per 1 % area, h) at 6, 10, 14, and 19 % per 1 % area. Maximum concentrations are the small numbers in each figure.

The poles to $\{01\bar{1}2\}$ or e-lamellae form a partial girdle perpendicular to the fold hinge, with two maxima symmetrically disposed about the long axes of the fibers in the outer arc and at the suture (Fig. 13). There is a progressive increase in the angle between the maxima and the fiber long axes (FL in Fig. 13) from outer arc to suture, the rotation of each maximum over this distance being about 20° . From suture to intrados the maxima continue to rotate away from FL, but the change is abrupt rather than smooth, and the end result is a point maximum of poles to $\{01\bar{1}2\}$ roughly normal to FL. Towards the intrados, bent twins, kinked twins, and twins in twins are also common.

The optic axes or $[0001]$ directions are similar to poles to $\{01\bar{1}2\}$ in their pattern of distribution. In the outer arc they form a partial girdle with two maxima in the profile plane of the fold although, unlike the situation for $\{01\bar{1}2\}$ poles, the girdle is populated between the maxima at FL. The maxima at the outer arc and at the suture make smaller angles with FL than do the maxima of poles to $\{01\bar{1}2\}$, but the rotation from outer arc to suture is

the same, roughly 20° . There is a similar abrupt transition from suture to intrados resulting at the latter location in a small circle centered on the normal to the fibers with an opening angle of about 25° (Fig. 13). Thus there is an abrupt appearance of nearly fiber-parallel twins and fiber-normal $[0001]$ directions between the suture and the intrados. These orientations are also locally observed in fibers in the outer arc.

In interpreting these fabric patterns, we must take into account the initial fabric in the veins and the deformation associated with buckling. It is important to note that the initial fabric would have been symmetrical about the suture, because the vein is antitaxial. Thus the present asymmetry is a result of deformation. We can infer the initial state by looking at the least deformed parts of the fold. The folding analysis led to the conclusion that the vein buckled to high amplitude to a large degree by pressure-solution removal of material from the intrados (Fig. 10). The neutral surface for the increment of deformation involving fold growth to high amplitude would thus have lain at or near the outer

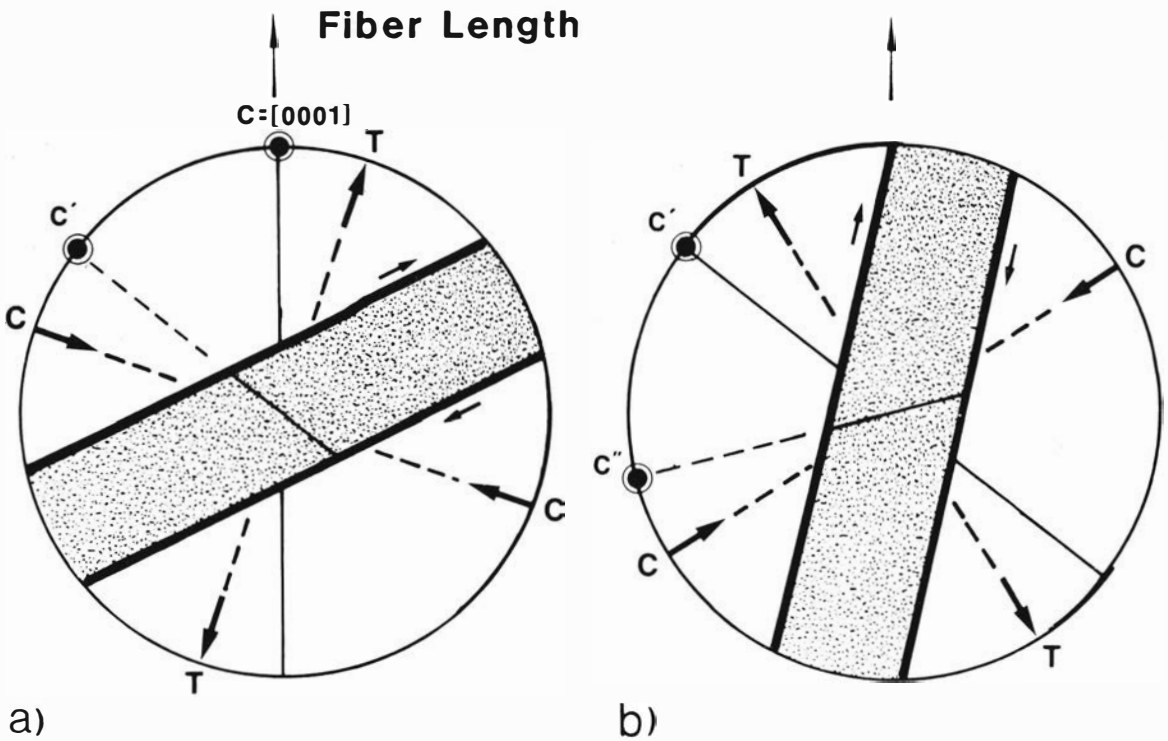


Fig. 14. Geometrical relationships involved with $\{01\bar{1}2\}$ twinning in calcite fibers with c-axis originally parallel to the fiber long axis. a) The initial state and first-developed twins, shown as stippled; $[0001]$ in the twin, c' , makes an angle of 52° to c . b) A later stage in which the host crystal is the twin of stage a), with $[0001]$ at c' , and a secondary twin has developed (stippled), for which $[0001]$ or c'' makes an angle of 52° to c' . C and T are the 'dynamic' axes of compression and tension developed for the twins of each case. Note that twins the mirror image of those shown (about a vertical line) are equally likely to develop as those shown.

arc of the fold, and the fibers least affected by buckling and most indicative of their pre-buckled state would be those adjacent to the outer arc, and those most affected by buckling and least indicative of their pre-buckled state would be in the intrados. This is consistent with the observations of twinning and pressure solution intensities. It should be noted that, because of the early stage of layer-parallel shortening, there will *not* be a neutral surface associated with the cumulative strain.

Fibers in the least-deformed outer arcs of the folds generally have length-parallel $[0001]$ (Fig. 13). This contrasts with the general view that the crystallographic directions of the crystals comprising fibers generally have no special orientation with respect to the length of the fiber (Ramsay and Huber, 1983, p. 236). Apparently, in the fold studied, fibers that were oriented with length-parallel $[0001]$ grew the fastest. Spry (1969, p. 161) has identified resulting fabrics of this type as columnar impingement textures. One might expect there to have been pro-

gressively more variation in $[0001]$ orientations from vein walls to the suture in the undeformed state. However, a broadening of the fabric pattern from outer arc to suture is not observed. It is thus likely that the predeformational fabric of the whole vein was one of $[0001]$ concentrated in the direction of the fiber long axes.

The only apparent modifier of the original fabric in the outer arc is twin gliding, and this does not alter the orientation of $[0001]$ in the host grains. The sense of twinning and resulting strains are consistent with their forming during the layer-shortening stage of buckling (Fig. 9). For a fiber with length-parallel c-axis, $\{01\bar{1}2\}$ would have made an angle of 26° with a layer-parallel σ_1 (Fig. 14), and thus have made an angle of 19° with the plane of highest resolved shear stress. The fabrics in the outer arc are consistent with twin gliding on conjugate sets producing the two maxima of $\{01\bar{1}2\}$ poles and leaving unaffected the initial pattern of a broad partial girdle of $[0001]$ axes.

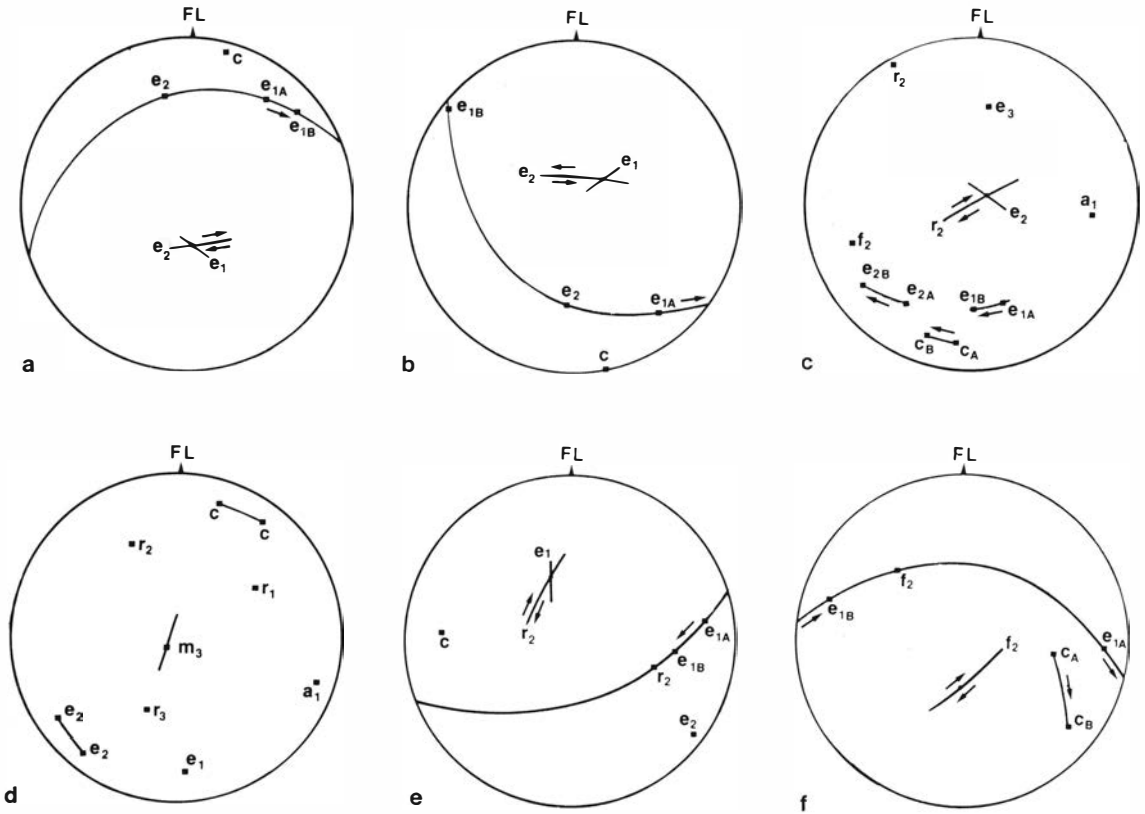


Fig. 15. Equal-area lower-hemisphere projections of internal and external rotations of $\{01\bar{1}2\}$ and $[0001]$. a) and b) Internal rotation of e_1 by twin glide on e_2 about an axis equal to the intersection of e_1 and e_2 [data for a) and b) were measured in domain C and hinge, from outer arc to suture, respectively]. c) External rotation of e_1 , e_2 , and c -axes by translation glide on r_2 about an axis equal to the intersection of r_2 and e_2 [data measured in domain B from outer arc to suture]. d) Possible external rotation of e_2 and c -axes by translation glide on a_1 about an axis equal to the pole of m_3 [data measured in domain C adjacent to suture]. e) Internal rotation of e_1 by translation glide on r_2 about an axis equal to the intersection of r_2 and e_1 [data measured in domain I adjacent to intrados]. f) External rotation of e_1 and c -axes by translation glide on f_2 [data measured in domain I. H. in intrados]. Squares = crystallographic axes or poles to crystallographic planes; subscripts A and B = initial and final positions of rotated feature respectively; double arrows = sense of slip on labeled glide plane; FL = fiber long axis.

The fabric patterns at the suture, similar to those at the outer arc with maxima rotated some 20° away from FL, suggest a similar development as at the outer arc, modified by some process related to the higher values of layer-parallel shortening in this location. Small internal and external rotations (Turner and Weiss, 1963, p. 337–338) of $\{01\bar{1}2\}$ and $[0001]$ were measured along the lengths of fibers from the outer arc towards the suture, and it appears that these are responsible for modifying the fabric.

What is the nature of these rotations? Translation gliding on a slip system will cause reorientation of any preexisting twins intersected by the glide plane. The axis of rotation of the pre-existing twin plane is

its intersection with the glide plane, and the poles of the rotated twin plane and active glide plane will be cozonal for all amounts of rotation (Turner et al., 1954a, p. 898). This is internal rotation, as the lattice of the host grain is not rotated. If internal rotation of earlier twins, say e_2 , occurs as a result of subsequent twinning, say e_1 , the pole to e_2 will migrate away from the pole to e_1 by 22° along the great circle e_1e_2 , and the e_1 lamellae will remain stationary. This is recorded in Fig. 15a and b.

Normally, slip on a glide system (which may cause internal rotations of elements intersected by the glide system), is accompanied by external rotation of the active glide system in the opposite sense to the internal rotation. Such external

rotations are necessary to cause the 20° change in orientation of [0001] noted between outer arc and suture (Fig. 13). For an external rotation within a single grain, the axis of rotation is normal to the deformation band (e.g. kink band) and it lies in the glide plane normal to the glide direction (Turner and Weiss, 1963, p. 337). This axis of external rotation can be determined graphically using two or more corresponding directions located in separate and differently oriented domains (Turner and Orozco, 1976), and it is the intersection of the great circles containing the mid-point of the arc connecting the unrotated and rotated directions and the pole of that arc. Using this graphical technique helped identify the translation mechanisms that externally rotated [0001] from the outer arc towards the suture, as positive slip on r and possibly slip on $a = \{1\bar{2}10\}$ (Fig. 15c and d).

Evidence for slip on r is given in Fig. 15c, in which we see that poles to both e_1 and e_2 and [0001] are rotated clockwise about an axis that approximates $[e_2:r_2]$, suggesting slip on r_2 . The axis of external rotation could possibly also lie in f_2 or a_1 . However, in our interpretation of fold development involving coaxial shortening normal to fiber lengths, r_2 would be oriented so as to have both the highest resolved shear stress and a sense of shear (positive) compatible with the observed rotations and applied stress. Positive slip on r_2 would rotate [0001] towards the normal to the length of the fibers and eliminate fiber-length parallel [0001]. The apparent lack of systematic rotation of e_3 in Fig. 15c is unresolved.

Evidence for possible slip on a is shown in Fig. 15d, in which rotations of e_2 and c are recorded. The bending of thick twins (approximately 10 microns or greater) points to either a_1 or c as possible slip planes, with a_1 more favorably oriented. The axis of external rotation and the slip direction approximate m_3 in $\{10\bar{1}0\}$ and [0001] respectively. This is compatible with the fibre-parallel extension expected during buckling. The sense of shear is indeterminate due to the lack of evidence of internal rotation. Slip on a_1 with the glide direction $[r_1:f_2]$ has been previously reported (Paterson and Turner, 1970), but it is rare.

In summary, there is good evidence that, to produce the fabric pattern measured at the suture, a fabric pattern very similar to that observed in the outer arc was modified by: 1) twinning (e.g. twin glide on e_2 after e_1), 2) positive translation on r , in which positive sense as defined by Turner et al. (1954a) is associated with rotations of [0001] towards the compression axis, and 3) possible translation on $a = \{1\bar{2}10\}$. The absence of fiber-length parallel [0001] at the suture is also accounted for by this.

Because a continuous transition of fabric from the suture to the intrados is not observed, a mechanism other than translation glide must be invoked to explain the intrados fabric. This mechanism must be twinning.

If calcite is twinned to completion the new [0001] will have rotated 52° from its original position towards the axis of compression (Fig. 14). If twinning to completion were the only mechanism to have affected the intrados fibers, [0001] maxima should be situated at 52° and 308° (c') in Fig. 13 (assuming [0001] was initially parallel to the fibers). If twinning to completion occurred twice, then [0001] maxima should be situated at 104° and 254° (c''), which is approximately what is observed. In this interpretation, the fiber-length-parallel 'twins' observed in the intrados are in fact the host grain, which has not quite been completely twinned a second time. The alternative explanation that they developed during folding as twins from host grains with c -axes at c' involves the wrong sense of slip for layer-parallel shortening. There is also evidence for translation glide in the intrados, and this has probably played a minor role in producing the observed fabric, as at the suture. Twinning to completion also explains the apparent decrease in the intensity of twinning in the intrados relative to the outer arc.

Translation glide continued after complete twinning of the fibers in the intrados, as there is isolated evidence of at least internal rotations of twin lamellae by slip on r_2 (Fig. 15e), where e_1 has rotated about its intersection with r_2 , and the poles to e_1 have migrated along the great circle e_1r_2 towards the pole to r_2 .

Removal of material by pressure solution in the intrados has locally been accompanied by intracrystalline slip. In one example, the bending of fibers by preferential dissolution was accommodated by slip on f_2 (Fig. 15f). In this particular fiber, slip planes are observed around a bend in the fiber. The poles to these slip planes are coincident with poles to f_2 . The axis of external rotation of [0001] and e_1 lies in f_2 . Bending occurred late as both fiber-length parallel e_1 and fiber-length normal [0001] are bent. The sense of rotation is negative, assuming the fibers were initially straight.

We have seen that both twinning on e and translation gliding on r , with minor slip on f and a when favourably oriented, have accommodated the layer-parallel shortening and fiber-parallel extension produced during buckling of the vein. These mechanisms worked interactively and intensified with increased strain to create the distinctive microfabric patterns measured along the suture and intrados. The observed symmetry of the microfabric should reflect the: 1) conditions and deformation mechan-

isms active during tectonism, 2) symmetry of applied stresses, and 3) the initial fabric (Turner and Weiss, 1963, p. 349). The orthorhombic symmetry of [0001] measured along the suture compares well with experimental and theoretically predicted symmetries of [0001] formed in limestones deformed in plane strain at 300–600°C, compressed perpendicular to an initial preferred microfabric, by twinning on *e* and translation glide on *r* (Turner et al., 1954; Wagner et al., 1982). However, the symmetry of [0001] in the intrados compares better with experimental and theoretically predicted [0001] symmetries formed in limestones deformed in either plane strain at 200–400°C, predominantly by twinning with minor slip, or with limestones deformed by axisymmetric compression by both twinning and translation gliding (Wagner et al., 1982).

Discussion and Conclusions

The buckled calcite vein lies at a small angle to cleavage (Figs. 1 and 2) and, whatever the deformation path experienced by the rock mass as a whole, the plane of the vein would most probably have experienced a non-coaxial strain history. However, there is little evidence in the fabric of the vein to indicate this. On the contrary, the fact that the fibers of the vein maintained their orthogonal attitude to the vein walls and the suture indicates that the vein experienced a largely coaxial strain history, which the crystallographic fabric reflects. Because the vein is competent, it would have acted as a stress guide, and whatever the stresses applied to the boundary of the vein during the deformational history, principal stresses within the vein would have tended to be parallel and perpendicular to the walls. The evidence of the crystallographic fabric is that the vein experienced a layer-parallel shortening before significant folding, and that folding to high amplitude was accommodated by further intracrystalline strain (largely twinning), of 'tangential longitudinal' orientation, accompanied by significant pressure solution. Both mechanisms increased in intensity towards the intrados of the fold. Pressure solution was intense enough that the antitaxial suture was only slightly deflected from its central position, contrary to the predictions of tangential longitudinal strain, and the neutral surface for the folding increment of deformation was very near the outer arc of the fold.

The folds have all the characteristics of buckles, and analysis of the distribution of wavelength/thickness ratios (*L*) and early layer-parallel shortening (*T*), in terms of single layer buckling theory, lead to

the conclusion that buckling of the calcite layer followed a highly non-linear flow law. A power law exponent of at least 3 and more probably > 10 for calcite is required to satisfy the fold data. This is consistent with the analysis of microfabric and experimental work on deformation of calcite. Deformation has been accommodated by intracrystalline twin and translation glide, and by pressure solution. During the early stage of buckling, twin glide was probably the dominant mechanism (as best preserved in the outer arc of the fold). Indeed, pressure solution was probably only important during later growth of the folds to high amplitudes. The power-law exponent for steady-state creep by intracrystalline flow in limestones or marbles has been found experimentally to be about 8 at temperatures of 500–800°C and strain rates of 10^{-3} – 10^{-7} /s by Heard and Raleigh (1972), and to be about 16 at 400–500°C and strain rates of 10^{-3} – 10^{-8} /s by Rutter (1974). Pressure solution leads to a linear dependence of strain rate on stress (Elliott, 1973; Rutter, 1976), although Fletcher (1982) has shown that buckling accommodated by diffusional mass transfer across the competent layer is a non-linear phenomenon. In any case it is unlikely that pressure solution was important during the early wavelength-selection stage of folding.

No independent estimate of pressure and temperature are available for the rocks from which the studied folds came. Hudleston and Holst (1984) postulated temperatures of 200–350°C during tectonism that produced the slates in the region. Both twinning on *e* and translation gliding on *r* can be active at these temperatures (Carter, 1976). Translation glide becomes relatively more favorable as temperature is increased (Wagner, et al., 1982). It is most unlikely, however, that there was a temperature difference between the suture and the intrados during fold formation that facilitated the activation of different deformation mechanisms. There would have been however, a stress gradient across the layer and the higher stresses in the intrados would have been more likely to have activated translation glide on *r*. It also seems likely that, as strain increased and grains became progressively more twinned, translation glide became activated on favorably oriented slip planes. The local stress distribution was probably highly inhomogeneous, leading to stress concentrations sufficient to activate glide.

The major controls on the [0001] fabric pattern were the initial preferred alignment of [0001] and twinning. The striking differences in the fabric pattern across the fold are due to variations in strain intensity, not to a change in deformation mechanisms. It is, however, interesting that mechanisms

other than twinning (translation gliding and pressure solution) contribute more to the deformation as strain intensity increases although they are of minor importance in contributing to the crystallographic fabric. If the fabric patterns observed were from a large structure whose fold-like form could not be directly observed, interpretation of these fabrics might be very different, and incorrect.

Acknowledgements. – The authors are most grateful to the reviewers, Angel Fernandez, Neil Mancktelow and Harro Schmeling, whose critical reviews have resulted in a greatly improved manuscript.

REFERENCES

- Biot, M.A. 1961: Theory of folding of stratified viscoelastic media and its implications in tectonics and orogenesis. *Bull. Geol. Soc. Am.* 72, 1595–1620.
- Carter, N.L. 1976: Steady state flow of rocks. *Rev. Geophys. Space Phys.* 14, 301–360.
- Elliott, D. 1973: Diffusion flow laws in metamorphic rocks. *Bull. Geol. Soc. Am.* 84, 2645–2664.
- Fletcher, R.C. 1974: Wavelength selection in the folding of a single layer with power-law rheology. *Am. J. Sci.* 274, 1029–1043.
- Fletcher, R.C. 1982: Coupling of diffusional mass transport and deformation in a tight rock. *Tectonophysics* 83, 275–291.
- Fletcher, R.C., & Sherwin, J. 1978: Arc lengths of single layer folds: a discussion of the comparison between theory and observation. *Am. J. Sci.* 278, 1085–1098.
- Groshong, R.H., Jr. 1972: Strain calculated from twinning in calcite. *Bull. Geol. Soc. Am.* 83, 2025–2038.
- Groshong, R.H., Jr. 1974: Experimental test of least-squares strain gage calculation using twinned calcite. *Bull. Geol. Soc. Am.* 85, 1855–1864.
- Heard, H.C., & Raleigh, C.B. 1972: Steady-state flow in marble at 500–800°C. *Bull. Geol. Soc. Am.* 83, 935–956.
- Hudleston, P.J. 1973: An analysis of single layer folds developed experimentally in viscous media. *Tectonophysics* 16, 189–214.
- Hudleston, P.J. 1986: Extracting information from folds in rocks. *J. Geol. Education* 34, 237–245.
- Hudleston, P.J. & Holst, T.B. 1984: Strain analysis and fold shape in a limestone layer and implications for layer rheology. *Tectonophysics* 106, 321–347.
- Lister, G.S., and Williams, P.F. 1983: The partitioning of deformation in flowing rock masses. *Tectonophysics* 92, 1–33.
- Nadai, A. 1963: *Theory of flow and fracture of solids*. vol. 2. McGraw-Hill, New York, 705 pp.
- Paterson, M.S. 1987: Problems in the extrapolation of laboratory rheological data. *Tectonophysics* 133, 33–43.
- Paterson, M.S., & Turner, F.W. 1970: Experimental deformation of constrained crystals of calcite in extension. In: *Experimental and Natural Rock Deformation* (edited by Paulitsch, P.). Springer-Verlag, Berlin, 109–141.
- Ramberg, H. 1961: Relationship between concentric longitudinal strain and concentric shearing strain during folding of homogenous sheets of rock. *Am. J. Sci.* 257, 382–390.
- Ramberg, H. 1963: Strain distribution and geometry of folds. *Bull. Geol. Inst. Univ. Uppsala* 42, 1–20.
- Ramsay, J.G. 1967: *Folding and fracturing of rocks*. McGraw-Hill, New York, 568 pp.
- Ramsay, J.G., & Huber, M. 1983: *The techniques of modern structural geology*. vol. 1, strain analysis. Academic Press, London, 307 pp.
- Rutter, E.H. 1974: The influence of temperature, strain rate and interstitial water in the experimental deformation of calcite rocks. *Tectonophysics* 22, 311–334.
- Rutter, E.H. 1986: The kinetics of rock deformation by pressure solution. *Phil. Trans. R. Soc. Lond. A* 283, 203–219.
- Sherwin, J., & Chapple, W.M. 1968: Wavelength of single-layer folds: a comparison between theory and observation. *Am. J. Sci.* 266, 167–179.
- Spry, A. 1967: *Metamorphic textures*. Pergamon Press, Oxford, 350 pp.
- Turner, F.J. 1953: Nature and dynamic interpretation of deformation lamellae in calcite of three marbles. *Am. J. Sci.* 251, 276–298.
- Turner, F.J., Griggs, D.T., & Heard, H. 1954: Experimental deformation of calcite crystals. *Bull. Geol. Soc. Am.* 65, 883–934.
- Turner, F.J., & Orozco, M. 1976: Crystal bending in metamorphic calcite, and its relations to associated twinning. *Contrib. Min. Pet.* 57, 83–97.
- Turner, F.J., & Weiss, L.E. 1963: *Structural analysis of metamorphic tectonites*. McGraw-Hill, New York, 545 pp.
- Wagner, F., Wenk, H.R., Kern, H., Van Houtte, P., & Esling, C. 1982: Development of preferred orientation in plane strain deformed limestone: experiment and theory. *Contrib. Min. Pet.* 80, 132–139.